Suppression of α-catenin and adherens junctions enhances epithelial cell proliferation and motility via TACE-mediated TGF-α autocrine/paracrine signaling

Eric N. Bunker†, Graycen E. Wheeler†, Douglas A. Chapnick, and Xuedong Liu*
Department of Biochemistry, University of Colorado, Boulder, CO 80303

ABSTRACT **Sustained cell migration is essential for wound healing and cancer metastasis. The epidermal growth factor receptor (EGFR) signaling cascade is known to drive cell migration and proliferation. While the signal transduction downstream of EGFR has been extensively investigated, our knowledge of the initiation and maintenance of EGFR signaling during cell migration remains limited. The metalloprotease TACE (tumor necrosis factor alpha converting enzyme) is responsible for producing active EGFR family ligands in the via ligand shedding. Sustained TACE activity may perpetuate EGFR signaling and reduce a cell's reliance on exogenous growth factors. Using a cultured keratinocyte model system, we show that depletion of α-catenin perturbs adherens junctions, enhances cell proliferation and motility, and decreases dependence on exogenous growth factors. We show that the underlying mechanism for these observed phenotypical changes depends on enhanced autocrine/paracrine release of the EGFR ligand transforming growth factor alpha in a TACE-dependent manner. We demonstrate that proliferating keratinocyte epithelial cell clusters display waves of oscillatory extracellular signal–regulated kinase (ERK) activity, which can be eliminated by TACE knockout, suggesting that these waves of oscillatory ERK activity depend on autocrine/paracrine signals produced by TACE. These results provide new insights into the regulatory role of adherens junctions in initiating and maintaining autocrine/paracrine signaling with relevance to wound healing and cellular transformation.**

Monitoring Editor
Kunxin Luo
University of California, Berkeley

Received: Aug 28, 2019
Revised: Dec 15, 2020
Accepted: Dec 18, 2020

INTRODUCTION

Wound healing in mammalian skin tissues is a highly complex and well-orchestrated reparative response that mainly involves four cell types (endothelial cells, fibroblasts, macrophages, and keratinocytes) that perform their roles in a stepwise manner (Gurtner *et al.*, 2008). The central players in this process are keratinocytes, which form a protective layer of extracellular matrix and intercellular junctions (Brandner *et al.*, 2010). The basal layer of keratinocytes divides at a rate capable of completely replenishing the tissue every 2 wk, resulting in outer layers that eventually dissipate into the environment (Fuchs and Raghavan, 2002). The epithelium not only

This article was published online ahead of print in MBoC in Press (http://www.molbiolcell.org/cgi/doi/10.1091/mbc.E19-08-0474) on December 30, 2020.

†Co–first author.

Author contributions: E.N.B., G.E.W., and D.A.C. developed the codes for data analysis. E.N.B., G.E.W., D.A.C., and X. L. performed the experiments. E.N.B., G.E.W., and X. L. designed the studies. E.N.B., G.E.W., and X. L. wrote the manuscript.

Competing interests: X.L. and the University of Colorado–Boulder have a financial interest in development of HDAC inhibitors for therapeutics and own equity in OnKure. X.L. is a cofounder and member of the board of directors of OnKure, which has licensed proprietary HDAC inhibitors from the University of Colorado–Boulder. OnKure has neither involvement in the experimental design nor funding of this study.

*Address correspondence to: Xuedong Liu (liux@colorado.edu).

Abbreviations used: ADAM, A disintigrin and metalloprotease; EdU, 5-ethynyl-2′-deoxy-uridine; EGF, epidermal growth factor; EGFR, epidermal growth factor receptor; EKAR, ERK kinase activity reporter; ELISA, enzyme-linked immunosorbent assay; ERK, extracellular signal–regulated kinase; FRET, Förster resonance energy transfer; HB-EGF, heparin-binding EGF-like growth factor; MMP, matrix metalloprotease; TACE, TNF-α converting enzyme; TGF-α, transforming growth factor alpha; TNF-α, tumor necrosis factor alpha; TSen, TACE sensor.

proliferates at a high rate but must remain primed for increased growth and motility when the tissue sustains a wound (Gurtner *et al.*, 2008). Once a wound is detected, cells on the edge of the wound stimulate closure and repair by propagating growth and motility signals to other cells nearby (Pastar *et al.*, 2014). Proliferation signaling is not required for wound closure in keratinocytes (Wickert *et al.*, 2016), but many of the stimuli and cell signaling pathways that control proliferation overlap with those that control growth and motility (Tanimura and Takeda, 2017).

One key signaling pathway that controls keratinocyte proliferation and migration is the epidermal growth factor receptor (EGFR) pathway. EGFR can be activated by a family of ligands that include epidermal growth factor (EGF), transforming growth factor alpha (TGF-α), heparin-binding EGF-like growth factor (HB-EGF), amphiregulin, betacellulin, and epiregulin (Harris *et al.*, 2003). All of these ligands are synthesized as membrane-anchored pro-forms and processed into bioactive soluble factors that bind EGFR (Blobel, 2005). This binding event causes dimerization and transautophosphorylation of the receptor, resulting in sequential activation of Ras, Raf, MEK, and extracellular signal–regulated kinase (ERK) to induce phosphorylation of myriad proteins and transcription factors critical for cell motility, proliferation, and survival. The EGF family of ligands are produced in the inactive pro-form and are converted by matrix metalloproteases (MMPs) and A disintegrin and matrix metalloproteases (ADAM_s) via proteolytic cleavage (Blobel, 2005). ADAM17, also known as the tumor necrosis factor alpha (TNF-α) converting enzyme (herein referred to as TACE), is known to cleave an array of EGFR pro-ligands, such as HB-EGF, amphiregulin, and TGF-α (Lee *et al.*, 2003; Scheller *et al.*, 2011). As such, TACE has been implicated in the survival and motility of epithelial cells, and its deletion in mice causes severe defects in skin, hair, eye, and organ formation (Peschon *et al.*, 1998). The effect of TACE and EGFR signaling on epithelial cell migration during wound healing is well documented (Miller *et al.*, 2013; Aoki *et al.*, 2017), but the signal(s) that causes TACE to activate ligand shedding and EGFR signaling remain poorly characterized. Because EGFR ligands are depleted continuously in target cells, our knowledge of how migrating cells maintain a steady supply of ligands to sustain EGFR signaling during cell migration is still limited.

Here, we show that loss of α-catenin, a component of cell adherens junctions, causes a large increase in TACE-mediated ligand shedding of EGFR ligand TGF-α and in cell motility. Using a new TGF-α shedding biosensor, we demonstrate that blocking TACE activity suppresses TGF-α release from cells and causes it to accumulate on the cell surface. Using live-cell imaging with Förster resonance energy transfer (FRET) biosensors reporting TACE and ERK activity, we further demonstrate that EGFR signaling can elevate TACE activity to form an autocrine signaling loop to sustain the release of TGF-α. The proliferating and migrating keratinocyte cell clusters show waves of oscillatory ERK activity, which require TACE activity. Our results suggest that the perturbation of cell–cell junctions promotes growth factor–independent cell proliferation and migration via elevated TACE-mediated TGF-α shedding and EGFR activation.

RESULTS

EGF stimulates activation of TACE and ERK to enable a positive feedback loop for autocrine signaling

Because TACE is responsible for the production of active EGFR ligands, we wanted to test whether TACE activity is spatially and temporally regulated in keratinocytes. We have previously developed a FRET-based TACE biosensor, TSen (Chapnick *et al.*, 2015), which allows us to employ quantitative live-cell imaging to reveal spatially sequestered TACE activity in cell populations and provide the temporal resolution necessary for measuring possible feedback between ERK and TACE. HaCaT keratinocytes stably expressing either TSen or an ERK activity reporter (EKAR) (Harvey *et al.*, 2008) were created.

As expected, EGF treatment of HaCaT EKAR cells leads to rapid and strong activation of ERK, and this activation is abrogated by treatment with the EGFR kinase inhibitor gefitinib, indicating that EGF-induced activation of the EKAR signal requires EGFR kinase activity (Figure 1A). The sample treated with vehicle (dimethyl sulfoxide [DMSO]) to reflect the basal activity of ERK demonstrates a slight increase in EKAR activity upon vehicle addition. Gefitinib suppresses ERK activity beyond the basal level, suggesting that EGFR is active in proliferating cells at the basal state. Cotreatment with EGF and BMS-561392 (BMS), a specific TACE inhibitor (Grootveld and McDermott, 2003), results in a slight delay in the activation of EKAR but does not affect the magnitude of the response. In parallel, HaCaT TSen cells were also exposed to EGF alone or in combination with gefitinib or BMS (Figure 1B). EGF treatment elevates TACE activity, as indicated by an increase in the inverse FRET ratio. The increase in TACE activity after EGF treatment is suppressed to basal levels by gefitinib or below basal levels by BMS. Therefore, this pair of FRET biosensors can faithfully report ERK and TACE activity in these cells.

Previous studies have shown that TACE is responsible for shedding of the soluble EGFR ligand TGF-α and that phosphorylation of TACE by ERK promotes its accumulation on the cell surface, presumably leading to higher ligand shedding capability (Borrell-Pagès *et al.*, 2003). This reciprocal regulation should produce an autocrine signaling–based positive feedback system (Shvartsman *et al.*, 2002). To experimentally determine the existence of an autocrine signaling loop between EGFR and TACE in proliferating and EGF-stimulated HaCaT cells, we conducted medium washout experiments in which ERK and TACE activities were monitored. Cells were preconditioned in HaCaT growth medium containing phosphate-buffered saline (PBS) as a vehicle control. After 1 h, this was exchanged for fresh medium containing DMSO, EGFR kinase inhibitor gefitinib, or a TACE inhibitor (either BMS or pan-MMP inhibitor TMI-1) at time zero (Figure 1C, left panel). After an initial drop in ERK activity, HaCaT EKAR cells are able to regain and sustain ERK activity after washout with replacement medium containing DMSO. However, if an EGFR or TACE inhibitor is included in the replacement medium, ERK activity remains low after washout. This result suggests that EGFR and TACE are both required for maintaining ERK activity in the absence of a stimulus.

Next, we performed an identical experiment but pretreated cells with medium containing EGF rather than PBS (Figure 1C, right panel). After 1 h, this was exchanged for medium containing the indicated treatment and no EGF. As expected, EGF-pretreated cells retain higher ERK activity after washout unless the replacement medium contains gefitinib. In the presence of either TACE inhibitor, ERK activity trends downward after 4 h compared with ERK activity after treatment vehicle, suggesting that TACE activity is required for sustained ERK activity after withdrawal of an EGF stimulation.

A reciprocal experiment with the TACE FRET sensor TSen was conducted (Figure 1D). HaCaT TSen cells were stimulated with EGF for 2 h before medium exchange with EGF-free medium containing vehicle (DMSO), gefitinib, or BMS at time zero. A control condition was pretreated with medium containing PBS, which was exchanged

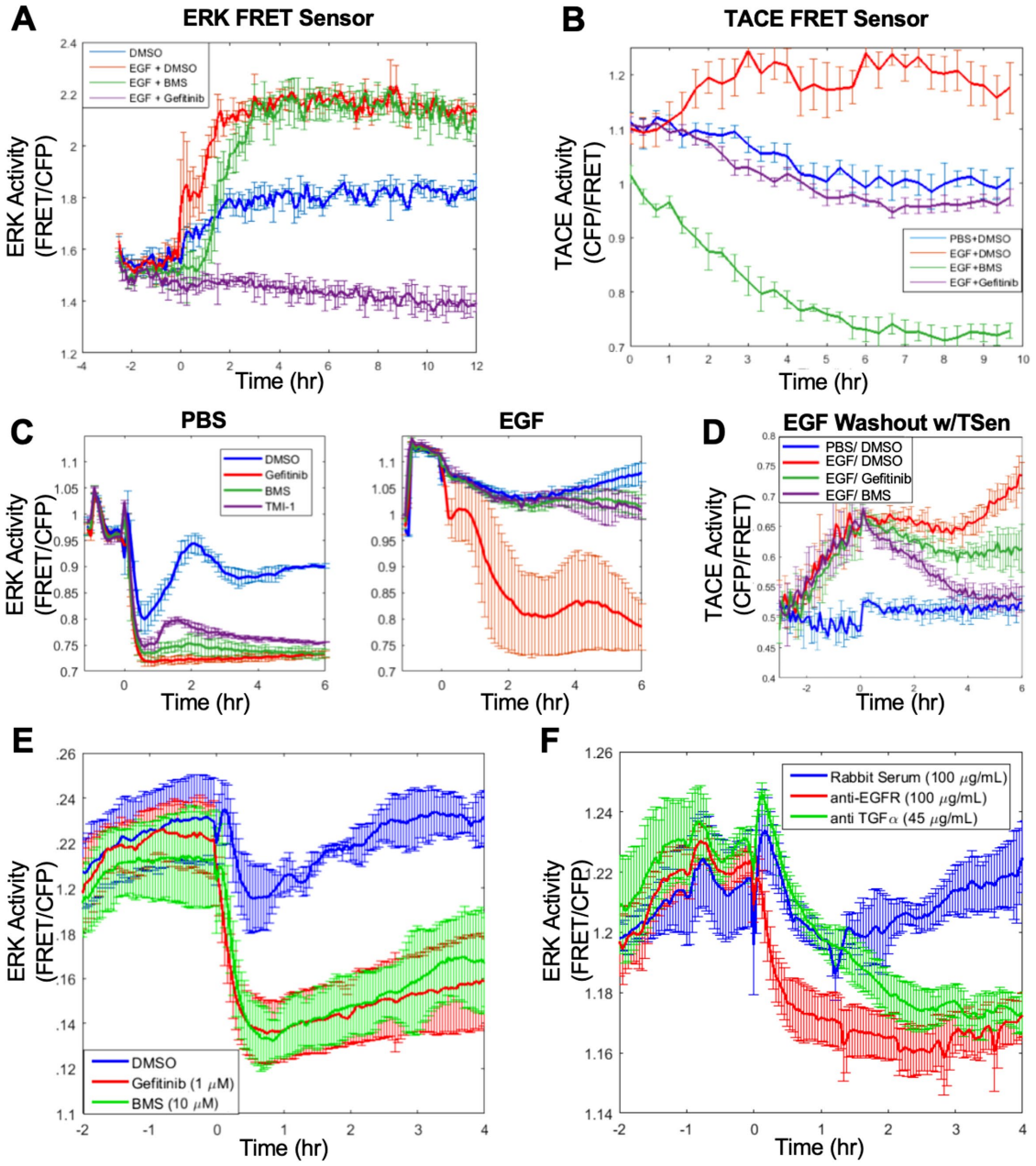

FIGURE 1: TACE and TGF-α are required for sustained autocrine ERK activity in HaCaT keratinocytes. (A, B) ERK and TACE activities in HaCaT keratinocytes. HaCaT cells stably expressing ERK FRET biosensor EKAR (A) or TACE FRET biosensor TSen (B) were stimulated with vehicle (DMSO), 10 μM EGF, 10 μM EGF plus 1 μM gefitinib (an EGFR inhibitor), or 10 μM EGF plus 10 μM BMS-561392 (BMS, a TACE inhibitor) for the indicated time. (C) EKAR-reported ERK activity in proliferating HaCaT cells after washout of EGF. Cells were treated with vehicle (PBS, left panel) or 10 μM EGF (right panel) for 1 h, followed by medium exchange for growth medium containing 1 μM gefitinib, 10 μM BMS, or 10 μM TMI-1 (a pan-MMP inhibitor). (D) Tsen-reported TACE activity in proliferating HaCaT cells after washout of EGF. Cells were pretreated for 2 h with medium containing vehicle (PBS) or 10 μM EGF followed by medium exchange for growth medium containing vehicle (DMSO), 1 μM gefitinib, or 10 μM BMS. (E) EKAR-reported ERK activity with EGFR or TACE inhibition by 1 μM gefitinib or 10 μM BMS, respectively. (F) EKAR-reported ERK activity with neutralizing antibodies for EGFR or TGF-α. The indicated treatments were added at 0 h. For all plots, experiments were performed in triplicate wells with more than 500 cells quantified in each replicate. Error bars represent SD.

for medium containing DMSO. Again, EGF elevates TACE activity, and this effect is partially abrogated by an EGFR inhibitor or completely eliminated by a TACE inhibitor. Collectively, these reciprocal experiments suggest that EGF stimulation engages an autocrine signaling loop in which both EGFR and TACE show elevated activities.

Autocrine signaling for sustained ERK activity requires TGF-α

In proliferating HaCaT monolayer cells, sustained ERK activity requires both EGFR and TACE, as an inhibitor targeting either enzyme suppresses ERK activity (Figure 1E). To determine whether TACE substrate TGF-α mediates the autocrine signaling cascade that

sustains ERK activity in proliferating cells, we added control serum, a neutralizing antibody to EGFR (cetuximab), or a neutralizing antibody to TGF-α to the growth medium and measured ERK activity (Figure 1F). Similar to gefitinib, cetuximab antagonizes ERK activity upon addition to the growth medium, while control serum has a minimal effect. The addition of a neutralizing TGF-α antibody suppresses ERK activity to the same extent as the EGFR-neutralizing antibody cetuximab but on a slightly delayed time scale. This result suggests that TGF-α is a key mediator of sustained ERK activity in proliferating HaCaT cells.

Development of a new TGF-α shedding biosensor for measuring TACE activity in medium and single cells

To study the TACE activity that is responsible for the shedding of the TGF-α ectodomain from cells, we developed a new TGF-α shedding biosensor in which the fluorescent protein mRuby2 and *Gaussia* luciferase (mGluc) were fused in tandem to the N-terminus of TGF-α adjacent to the known TACE proteolytic cleavage site (Harris *et al.*, 2003) (Figure 2A). This sensor enables us to study the TGF-α ectodomain in single cells using the mRuby2 signal and in bulk using mGluc. Previous studies have shown that insertion of the secretable alkaline phosphatase tag to TGF-α or HB-EGF or Epigen did not affect the shedding of these ligands by TACE, and such fusions are useful for detection and quantitation of the shed ligand form of these proteins in the medium (Sahin and Blobel, 2007; Le Gall *et al.*, 2009). One downside of alkaline phosphatase–tagged TGF-α or related EGF ligands is that it is not possible to track ligand shedding in single cells at high temporal resolutions. To overcome these limitations, we stably integrated the mRuby2-mGluc-TGF-α sensor into the genome of HaCaT cells.

MMP inhibition via TMI-1 treatment leads to a significantly lower level of mGluc signal in the conditioned media of HaCaT cells compared with cells treated with vehicle (DMSO) (Figure 2B), indicating that TACE is required for maximal cleavage of the mRuby2-mGluc-TGF-α sensor on the cell surface. Similarly, confocal imaging of HaCaT cells shows that basal cell surface accumulation levels of mRuby2-mGluc-TGF-α are almost undetectable, but mRuby2 signal can be seen at the cell surface or in intracellular vesicles when cells are treated with TMI-1 (Figure 2C), suggesting high basal levels of sensor cleavage. TACE inhibition via treatment with 10 μM BMS results in a steady increase of mRuby2 fluorescence on the cell surface, while the washout of BMS reduces mRuby2 signal on the cell surface (Figure 2D). Continuous exposure to either BMS or TMI-1 after washout allows cells to sustain high levels of mRuby2 fluorescence, suggesting that the TGF-α shedding biosensor is accurately reporting signaling dynamics of TACE activity in HaCaT cells. *Gaussia* luciferase signal in the media starts increasing within 1 h of EGF treatment and begins to decay within 200 min of TACE inhibition via TMI-1 treatment (Figure 2E). An enzyme-linked immunosorbent assay (ELISA) with TGF-α antibodies was used to compare TGF-α levels in the media of wild-type HaCaT cells and HaCaT cells expressing the TGF-α sensor (Figure 2F). The expression of the sensor did not significantly alter the effect of EGF or TMI-1 treatment on TGF-α levels.

TACE knockout cells are defective in proliferation and migration

The above studies strongly implicate TACE as a key player in EGFR-dependent autocrine signaling maintenance. To assess the importance of TACE in HaCaT cells, we used CRISPR/Cas9 to create stable cell lines devoid of TACE. We found that HaCaT cells lacking TACE did not expand in culture under normal conditions but instead require external growth factor stimulation. Supplementing the growth medium with EGF allowed us to generate a few TACE-null cell lines by clonal expansion from a CRISPR/Cas9-treated population. To ensure that the TACE knockout is specific, we created a TACE expression vector with scrambled silence mutations in the CRISPR/Cas9 target sequence and introduced it stably in TACE-null cell lines to generate a TACE rescue HaCaT cell line. Expression of TACE in wild-type, TACE-null, and rescue cell lines is as expected, as verified by Western blot analysis with an anti-TACE antibody (Figure 3A).

To investigate the effects of TACE loss on ERK signaling, we performed immunoblotting analysis using phospho-ERK (pERK) and ERK2 antibodies (Figure 3A). In agreement with a role for TACE in sustaining ERK activity, TACE-null cells show a marked reduction in pERK, and this defect is largely rescued by ectopic expression of TACE. Differences in pERK levels can be negated by treatment with TMI-1, suggesting that TACE is responsible for elevated pERK activity in proliferating HaCaT cells. Restoration of ERK activity upon TACE rescue was also confirmed with live-cell imaging of the EKAR sensor (Figure 3B).

Because TACE-null cells rely on external EGF for proliferation, we used an EdU (5-ethynyl-2′-deoxy-uridine) assay to measure the fraction of cells proceeding through the cell cycle within a 4-h period by measuring EdU incorporation to identify cells that had undergone S-phase. In the absence of EGF, TACE knockout cells have very little EdU incorporation, whereas wild-type and TACE rescue cells show robust EdU incorporation (Figure 3C). These results suggest that loss of TACE reduces ERK phosphorylation and causes a significant reduction in S-phase entry and consequently cell proliferation. Therefore, TACE activity is required for basal cell proliferation in HaCaT keratinocytes.

Our previous work shows that spatially constrained ERK activity drives the collective migration of keratinocytes (Chapnick and Liu, 2014). ERK activity linearly correlates with cell motility. To determine whether TACE activity is important for cell motility, we performed single-cell tracking experiments using a nuclear dye and the ImageJ TrackMate plug-in (Tinevez *et al.*, 2017) to assess changes in cellular motility in both TACE-null and rescue cells (Figure 3D). Motility speed is restored upon TACE rescue, supporting a role for TACE in cell migration (Maretzky *et al.*, 2011). Taken together, these results indicate that TACE is essential for cell proliferation and cell motility.

Loss of α-catenin elevates autocrine signaling and cell proliferation

Having established that an autocrine signaling loop involving EGFR and TACE is required to sustain ERK activation and TGF-α shedding, we next investigated what type of signals beyond growth factors can engage this autocrine signaling cascade. We demonstrated previously that depletion of α-catenin in HaCaT keratinocytes reduces cell adherens junctions, increases individual cell motility (particularly at low cell density), and decreases collective migration of epithelial sheets (Nardini *et al.*, 2016). The biochemical mechanisms that are responsible for these phenotypes are still not well understood. We hypothesized that the loss of α-catenin results in hyperactive autocrine signaling, which causes increased cell motility and proliferation.

To test this hypothesis, we generated a stable short hairpin RNA (shRNA) knockdown of α-catenin in HaCaT cells (Figure 4A). We observed a large morphological change accompanied by disruption of cell–cell junctions, revealing a mesenchymal morphology with loose connections as opposed to the tightly bound epithelial colonies seen in HaCaT cells expressing a nontargeting control shRNA

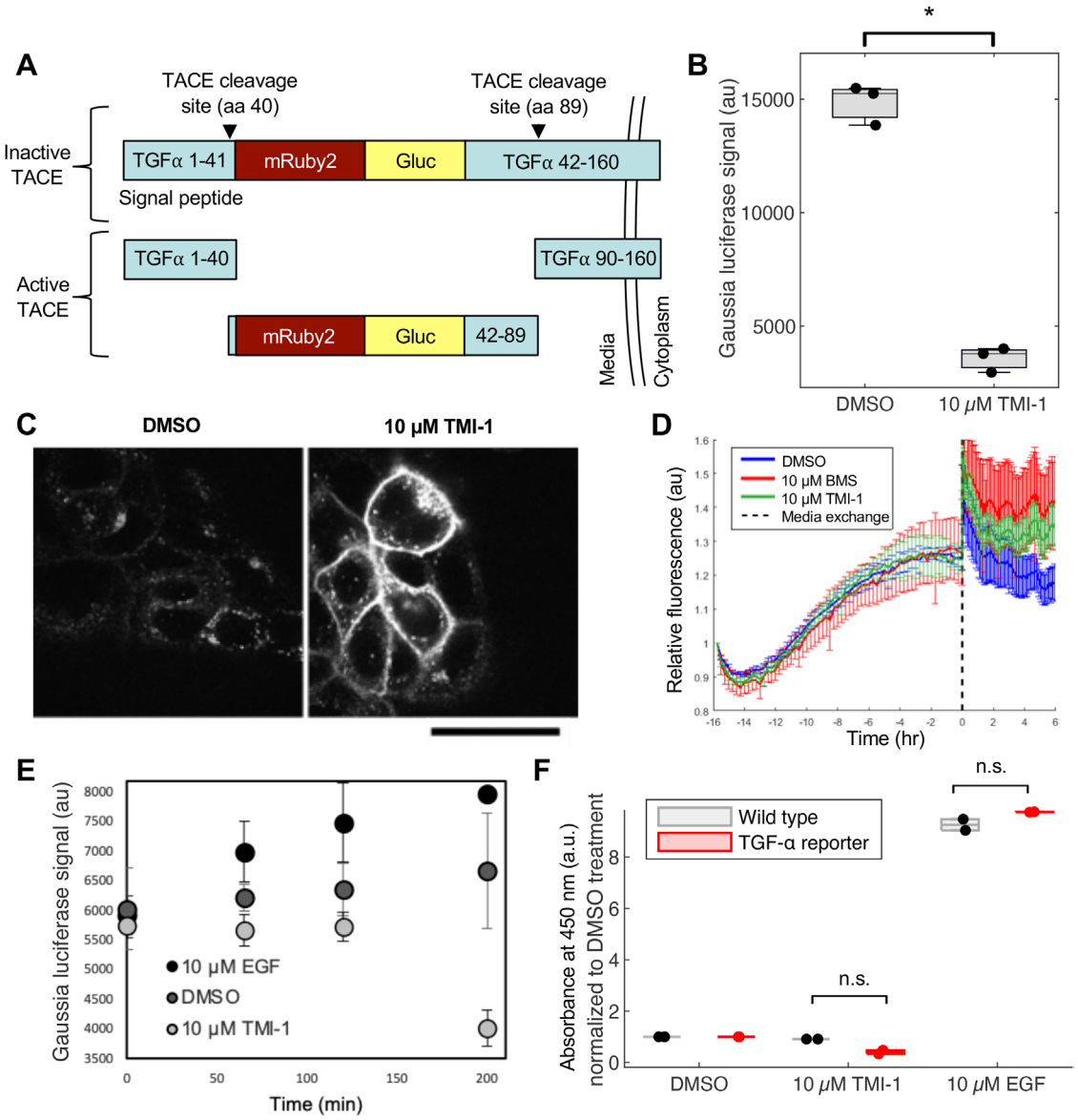

FIGURE 2: A new TGF-α shedding biosensor measures TACE shedding activity. (A) Schematic of chimeric TGF-α shedding reporter construct. mRuby2 and *Gaussia* luciferase were inserted between the signal sequence and the TACE cleavage site. (B) mGluc signal in medium of HaCaT cells stably expressing TGF-α shedding reporter was measured after treatment with vehicle (DMSO) or MMP inhibition with 10 μM TMI-1 for 18 h. Medium was extracted from biological triplicate wells. (C) Confocal imaging of HaCaT cells stably expressing TGF-α shedding reporter treated with vehicle or 10 μM TMI-1 for 18 h. Scale bar indicates 30 μm. (D) Washout experiment with TACE inhibitors. HaCaT TGF-α shedding reporter cells were treated with 10 μM BMS to inhibit TACE over a 16 h period until medium exchange at the indicated 0 time point, after which cells were incubated with vehicle, 10 μM BMS, or 10 μM TMI-1 for an additional 6 h. Relative mRuby2 fluorescence of cells was measured in triplicate wells and quantified for more than 500 cells in each condition. Error bars indicate SD. (E) HaCaT TGF-α shedding reporter cells were incubated with vehicle, 10 μM EGF, or 10 μM TMI-1 starting at time 0. *Gaussia* luciferase signal in the media was measured in biological duplicates for each condition at each time point. Error bars indicate SD. (F) Biological duplicates of wild-type HaCaT cells or HaCaT mR2-glucTGF-α reporter cells were incubated with vehicle, 10 μM EGF, or 10 μM TMI-1 for 18 h before TGF-α levels in the media were measured by ELISA. In all panels, *p* values were determined by two-tailed Student's *t* test. * $p \leq 0.0500$. Box plots show all data points with quartiles indicated.

(Figure 4B). The mesenchymal morphology seen in phase contrast images prompted us to investigate whether these cells had undergone epithelial to mesenchymal transition (EMT). TGF-β is a potent EMT inducer in epithelial cells, including HaCaT keratinocytes, which leads to a reduction in E-cadherin and up-regulation of c-Myc, slug, and vimentin (Xu *et al.*, 2009). Unlike TGF-β depletion, loss of α-catenin in HaCaT cells has little if any effect on E-cadherin expression, despite the loss of cell junctions and profound morphological changes. There are no discernible changes in N-cadherin, c-Myc, or slug in these cells, although vimentin levels are slightly elevated, which is consistent with the mesenchymal morphology (Figure 4A). Immunostaining of E-cadherin in control and α-catenin knockdown

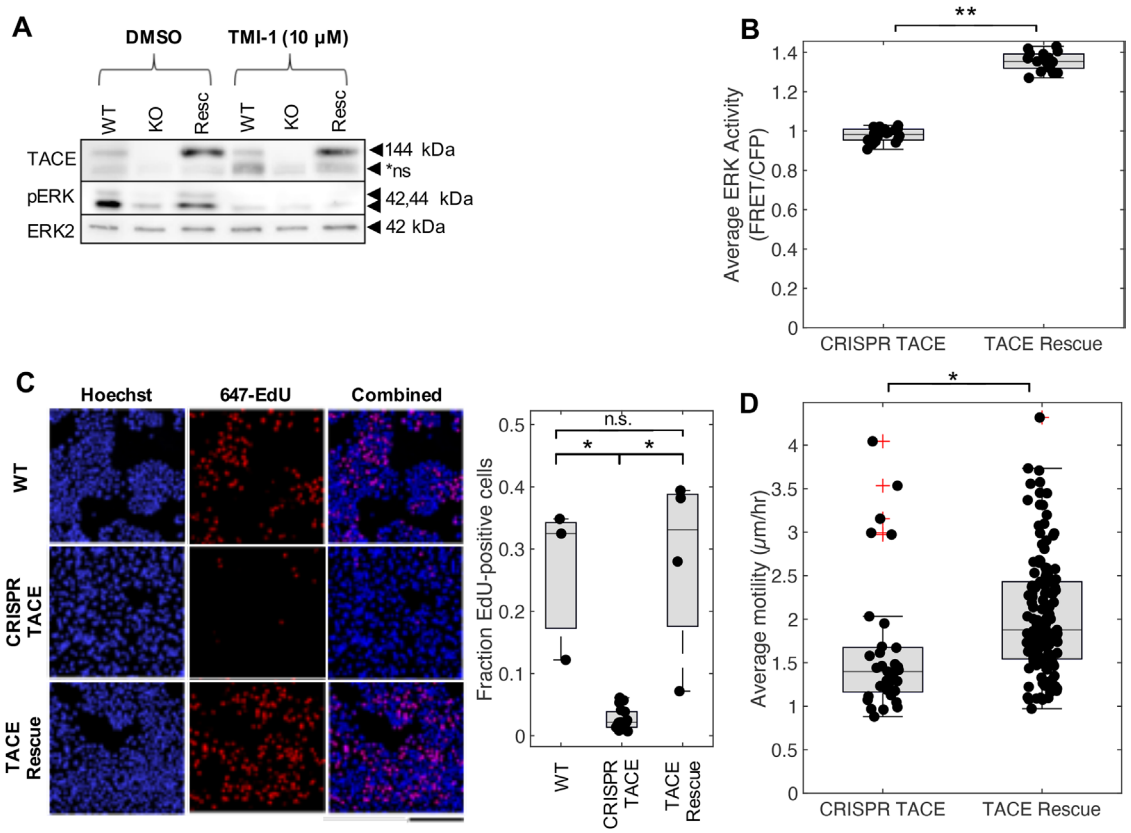

FIGURE 3: TACE knockout in HaCaT cells decreases ERK activity, cell proliferation, and cell migration. (A) Wild-type, CRISPR TACE knockout, and TACE rescue HaCaT cell lines were immunoblotted for pERK, total ERK2, and TACE protein levels after treatment with vehicle (DMSO) or MMP inhibitor TMI-1 (10 μM). Arrow indicates TACE; "ns" indicates a nonspecific band. (B) Basal ERK levels were measured at a single timepoint in CRISPR TACE knockout and TACE rescue HaCaT cells stably expressing the EKAR FRET reporter. Each measurement was performed in 18 replicate wells. (C) EdU incorporation experiment to measure proliferation of wild-type (top), CRISPR TACE knockout (middle), and TACE rescue (bottom) HaCaT cell lines. Hoechst dye (blue) was used to label all nuclei and EdU (red) to label cells that entered S-phase in a 4-h period. Scale bar indicates 500 μm. A custom MATLAB script was used to select wells with comparable densities between conditions for quantitative analysis. Three wells were quantified for wild-type, 18 for CRISPR TACE, and four for TACE rescue. (D) Migration of CRISPR TACE knockout and TACE rescue cells was measured in triplicate wells for 5 h with a time point every 20 min. The average motility across all time points was quantified for individual cells (34 total cells with at least eight cells/well for CRISPR TACE; 133 total cells with at least 39 cells/well for TACE rescue) using the ImageJ TrackMate plug-in as described in *Materials and Methods*. In all panels, p-values were determined for all data points (including outliers) by two-tailed Student's *t* test. * $p \leq 0.0500$, ** $p \leq 0.0100$. Box plots show all data points with quartiles indicated; red crosses denote outliers.

cells reveals that E-cadherin remains on the cell membrane even in cells with no adherens junctions (Figure 4C). A similar staining pattern is also observed for β-catenin (Figure 4D). Taken together, these results indicate that the loss of adherens junctions as a result of α-catenin depletion profoundly changes cell–cell interactions but does not induce full EMT.

Next, we determined whether the depletion of α-catenin enhances cell proliferation. Control and α-catenin knockdown cells were tested for EdU incorporation. α-Catenin knockdown cell populations have ~30% more EdU-positive cells than control cell populations, indicating a higher fraction of cells progressing through the cell cycle (Figure 4, E and F). This result is consistent with the idea that loss of α-catenin stimulates cell proliferation.

Loss of α-catenin activates TACE and causes increased motility and shedding of TGF-α

There are numerous ways for cells to become hyperproliferative; elevated ERK activity is known to be associated with this phenotype. Western blotting of pERK levels in control and knockdown cells confirmed elevated ERK activity in α-catenin knockdown cells (Figure 5A), but TACE protein levels in these knockdowns remain unchanged (Figure 6A). To further test whether loss of α-catenin results in higher ERK activity, we introduced EKAR or TSen to stable cell lines expressing either an α-catenin–targeting shRNA or a nontargeting scrambled shRNA. ERK and TACE activities were measured independently by EKAR and TSen, respectively, and our results show that α-catenin knockdown cells have higher average ERK and TACE activities than control cells (Figure 5, B and C). Consistent with this and our earlier finding that higher TACE and ERK activities are associated with cell motility (Figure 3D), α-catenin knockdown cells demonstrate an increased rate of motility compared with control cells (Figure 5D). To ensure that the relationship between α-catenin knockdown and ERK activity is not cell line–specific, we created stable cell lines expressing EKAR and either an α-catenin–targeting shRNA or a nontargeting scrambled shRNA in THCE, a telomerase-immortalized human corneal epithelial cell line, and NMuMG, a glandular epithelial cell line

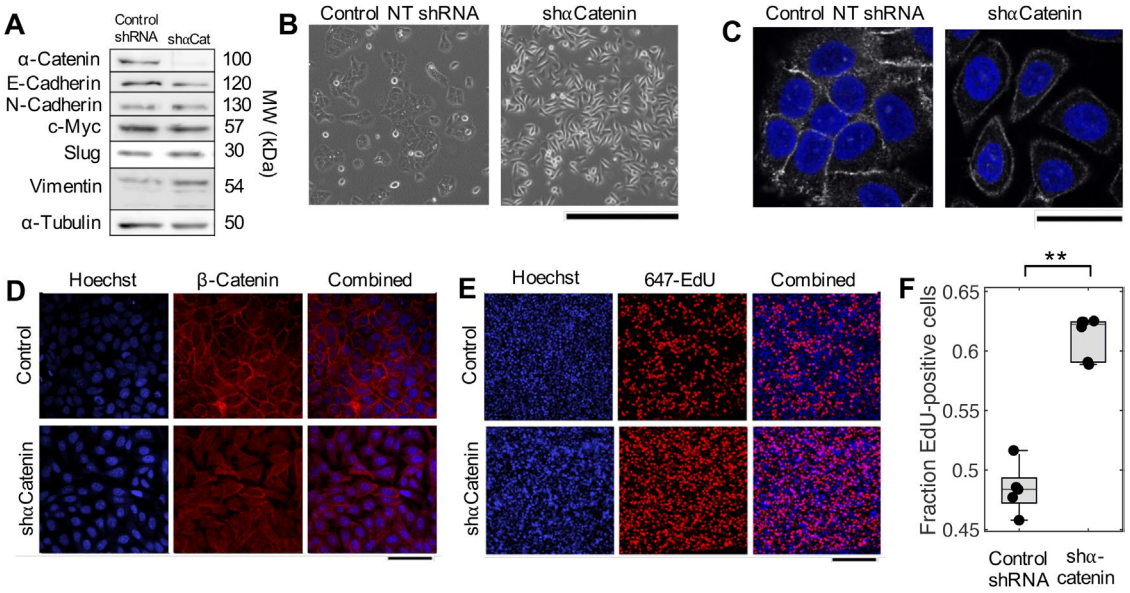

FIGURE 4: Loss of α-catenin disrupts adherens junction and leads to increased cell proliferation. (A) Western blot comparing cells expressing a nontargeting shRNA or an shRNA targeting α-catenin for 48 h. α-Tubulin was used as loading control. (B) Differential interference contrast images show the morphological change of α-catenin knockdown in HaCaT cells. Scale bar indicates 400 μm. (C) Immunofluorescence for E- cadherin shows that it remains at the membrane, but there are no cell–cell junctions. Scale bar indicates 30 μm. (D) Immunofluorescence of β-catenin shows that it has not translocated to the nucleus in response to α-catenin knockdown. Scale bar indicates 50 μm. (E, F) α-Catenin silencing causes a significant increase in cell proliferation in HaCaT cells. EdU incorporation experiments and analysis were performed as described in Figure 3C. Five wells were quantified for control, six for α-catenin knockdown. All images in panels B–E are identically contrasted between conditions. Scale bar indicates 500 μm. In all panels, *p* values were determined by two-tailed Student's *t* test. * $p \leq 0.0500$, ** $p \leq 0.0100$. Box plots show all data points with quartiles indicated.

from *Mus musculus*. ERK levels, as measured by EKAR, were higher in both of these α-catenin knockdown cell lines compared with their respective controls (Supplemental Figure S1).

Because we have shown that TGF-α is responsible for autocrine signaling that produces higher ERK activity in HaCaT cells (Figure 1E), we wanted to determine whether knockdown of α-catenin also leads to elevated shedding levels of TGF-α. To this end, we took advantage of our newly developed TGF-α shedding biosensor, mRuby2-mGluc-TGF-α. HaCaT cells stably expressing this TGF-α sensor and treated with the TACE inhibitor BMS showed progressively increasing cellular mRuby2 fluorescence until a medium exchange, upon which the cellular mRuby2 fluorescence decreased in the absence of BMS (Figure 2D). A medium exchange on either control or α-catenin knockdown cells revealed a more rapid depletion of mRuby2 fluorescence in the knockdown cells, indicative of a higher rate of TGF-α cleavage (Figure 5E). We then measured the luciferase signal in conditioned medium after 18 h of either DMSO or BMS treatment in both control and α-catenin knockdown cells (Figure 5F). Untreated α-catenin knockdown cells demonstrated more than 2.5-fold higher levels of TGF-α in the medium compared with control cells. This difference was negated by TACE inhibition via BMS treatment, which resulted in lower luciferase signal in both samples. Together, these results indicate that TACE activity appears to be significantly increased with α-catenin knockdown in HaCaT keratinocytes, resulting in elevated production of TGF-α to engage autocrine EGFR signaling.

TACE is required for elevated autocrine signaling upon loss of α-catenin

The hyperproliferative response associated with the loss of α-catenin could be a result of the hyperactivation of TACE (TACE downstream of α-catenin) or the release of inhibition of cell proliferation by α-catenin independent of TACE (TACE upstream of α-catenin). To distinguish between these two possibilities, we performed epistasis analysis between α-catenin and TACE in controlling cell proliferation responses. If TACE is required for the elevated autocrine signaling seen after α-catenin knockdown, we would expect that TACE-null cells should blunt the phenotypes associated with loss of α-catenin. To test this notion, we generated a stable α-catenin knockdown in our TACE knockout cells (Figure 6A). α-Catenin knockdown still causes a disruption of cell–cell junctions and an altered morphology in the absence of TACE (Figure 6B) but no longer leads to an increase in vimentin (Figure 6A). Subsequently, we assessed whether α-catenin knockdown was able to cause a hyperproliferative phenotype without TACE and discovered that both TACE-null cell lines had almost no cells progressing through the cell cycle in a 4-h period using an EdU incorporation assay (Figure 6C). This result indicates that loss of α-catenin induces hyperproliferation of keratinocytes and that this induction requires TACE activity.

We also measured the motility of TACE-null and TACE rescue cells expressing either an shRNA targeted to α-catenin or a scrambled control shRNA (Supplemental Figure S2). The motility of TACE rescue cells is increased by α-catenin knockdown and decreased when the activation of ERK is inhibited with CI-1040, a specific inhibitor for MEK, which signals directly upstream of ERK. The motility of TACE-null cells is not significantly affected by either α-catenin knockdown or MEK inhibition, indicating that TACE, ERK, and adherens junctions are all modulating motility along the same signaling axis.

To determine whether the elevated production of TGF-α seen in α-catenin knockdown cells (Figure 5E) is TACE-dependent, we stably expressed the TGF-α shedding biosensor in the TACE-null

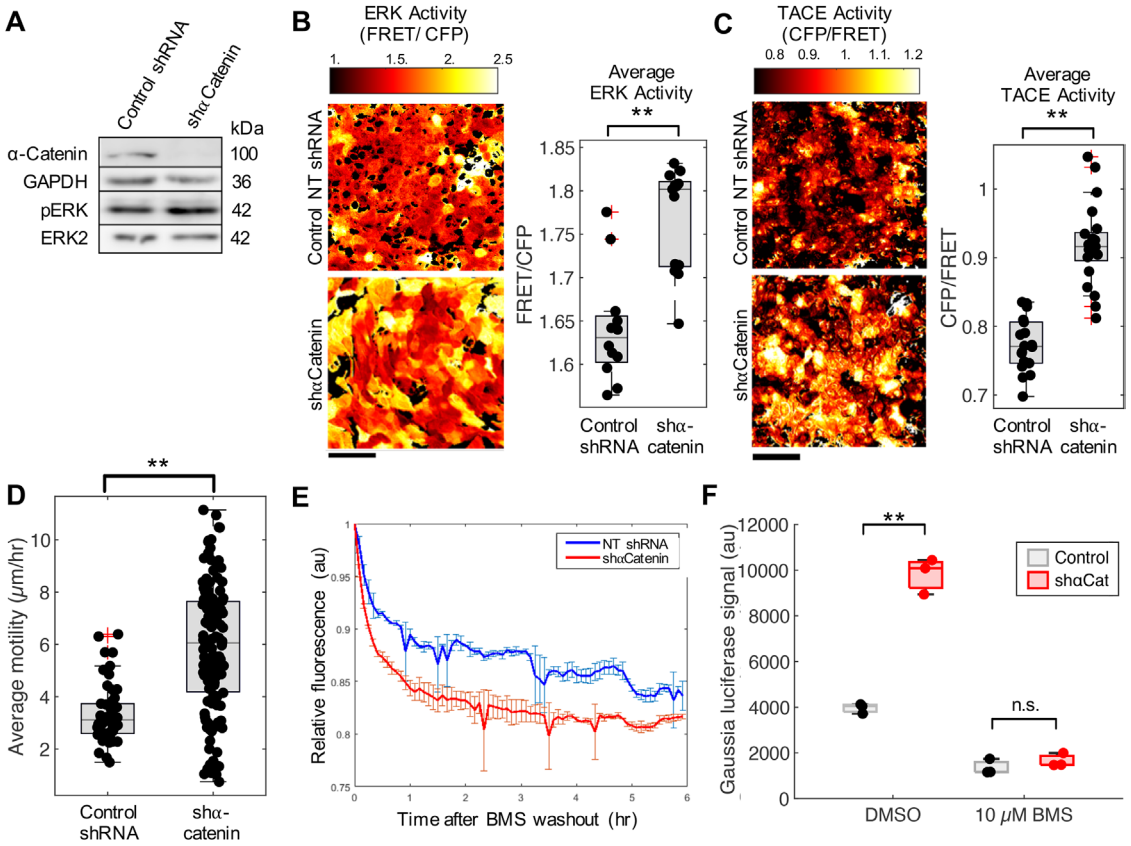

FIGURE 5: Loss of α-catenin increases ERK activity, motility, and TGF-α ligand shedding in HaCaT cells. (A) Western blot shows total ERK and pERK in control and α-catenin knockdown cells. (B, C) Images of HaCaT cells pseudocolored to indicate ERK (B) or TACE (C) activity, as measured by respective FRET biosensors in control and α-catenin knockdown cells. A custom MATLAB script was used to select wells with comparable densities between conditions for analysis. For B, 12 wells were quantified for control, 13 for α-catenin knockdown. For C, 18 wells were quantified for control, 21 for α-catenin knockdown. Scale bar indicates 80 μm. (D) Effect of α-catenin depletion on cell motility. Migration of wild-type or α-catenin knockdown HaCaT cells was measured for 5 h with a time point every 20 min. Average motility across all time points was quantified for individual cells (51 total cells with at least 15 cells/well for control cells; 140 total cells with at least 40 cells/well for α-catenin knockdown) using the ImageJ TrackMate plug-in as described in *Materials and Methods*. (E) Time course of mRuby2-Gluc-TGF-α cleavage in control and α-catenin knockdown cells upon washout of 10 μM BMS (TACE inhibitor). Error bars show SD. (F) Cleavage of mRuby2-Gluc-TGF-α in control and α-catenin knockdown HaCaT cells measured by *Gaussia* luciferase activity. Cells were seeded in a 96-well plate at 50,000 cells/well and then treated with 10 μM BMS or DMSO control for 18 h. Each measurement was performed in biological triplicates. In all panels, *p* values were determined by two-tailed Student's *t* test.** $p \leq 0.0100$. Box plots show all data points with quartiles indicated; red crosses denote outliers.

and TACE rescue cell lines with or without α-catenin knockdown and measured the shedding activity of mRuby2-Gluc-TGF-α with or without BMS treatment (Figure 6D). Without TACE, α-catenin knockdown cells secrete TGF-α at levels similar to those in control cells expressing a nontargeting shRNA, suggesting that the elevated TGF-α production associated with α-catenin depletion depends on TACE. In further support for this notion, the differences between control and α-catenin knockdown in TACE rescue cell lines were restored, and rescue cells were sensitive to TACE inhibition by BMS. Thus, our results support a model in which loss of α-catenin perturbs adherens junctions and consequently activates TACE to promote the production of TGF-α, which engages autocrine signaling and drives cellular proliferation and migration.

Pulsatile ERK activity in proliferating HaCaT keratinocytes requires TACE

Previous studies in single cells using live-cell reporters have shown that ERK activity occurs in discrete pulses in response to physiological levels of EGF or to serum (Albeck *et al.*, 2013; Aoki *et al.*, 2013; Regot *et al.*, 2014; Sparta *et al.*, 2015). To investigate whether ERK pulses also occur in proliferating keratinocytes, we imaged subconfluent HaCaT cells stably expressing the EKAR FRET biosensor grown in 10% serum for 4 h of treatment with vehicle (DMSO), 10 μM BMS, or 1 μM gefitinib added at 0 h (Figure 7A). Pulses of ERK activity (determined by the ratio of FRET to cyan fluorescent protein [CFP]) were counted in single cells (Figure 7B). EGFR inhibition via gefitinib treatment has previously been shown to block ERK activity pulses in epithelial cells (Sparta *et al.*, 2015). Consistent with past reports, virtually all ERK activity and ERK activity pulses in single cells are diminished upon EGFR inhibition. Treatment with a TACE inhibitor (BMS) prevents ERK activity and pulses in almost all cells shortly after BMS exposure; while some cells recover ERK activity after prolonged TACE inhibition, the activity levels are lower, and pulses occur far less frequently. This result suggests that TACE activity is at least partially responsible for pulsatile ERK activity in HaCaT cells, while EGFR activity is crucial.

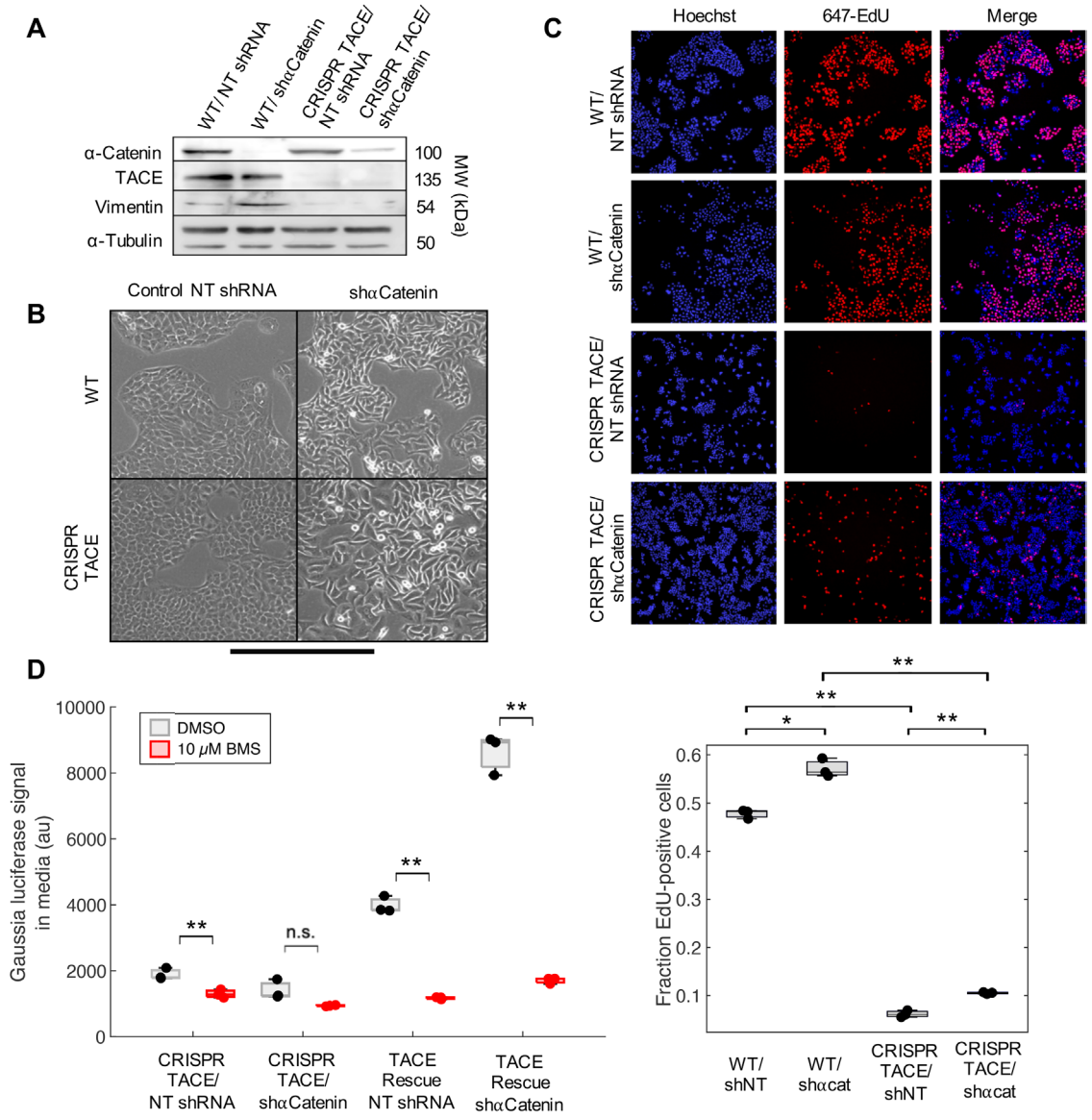

FIGURE 6: TACE is required for a hyperproliferative response and elevated autocrine production of TGF-α upon loss of α-catenin. (A) Western blot shows α-catenin knockdown in cells expressing TACE or with TACE knockout. α-Catenin knockdown in CRISPR TACE cells achieved α-catenin protein levels nearly as low as in cells with TACE but did not show an increase in vimentin. (B) Differential interference contrast images of α-catenin knockdown in wild-type (top) or TACE-null (bottom) cells showed that a morphological change after α-catenin silencing occurs in the presence or absence of TACE. Scale bar indicates 400 μm. (C) Hoechst dye (blue) was used to stain all nuclei; EdU stain (red) shows cells that entered S-phase in a 4-h period. Wild-type cells expressing either a nontargeting control or an shRNA for α-catenin (top two rows) show a large fraction of EdU-positive cells compared with TACE-null cells expressing either a nontargeting control or an shRNA for α-catenin (bottom two rows). Single-cell quantification shows a very low fraction of EdU-positive cells in the absence of TACE. At least 50 cells were quantified per image, performed in triplicate. Scale bar indicates 500 μm. (D) HaCaT cells expressing mRuby2- Gluc-TGF-α were seeded in a 96-well plate at 50,000 cells/well and then treated with 10 μM BMS or DMSO control for 18 h. Each measurement was performed in biological triplicates. In all panels, error bars indicate SD. *p* values were determined by two-tailed Student's *t* test. * $p \leq 0.0500$, ** $p \leq 0.0100$. Box plots show all data points with quartiles indicated.

Although TACE inhibitor BMS eliminates ERK pulses in HaCaT cells, the observed effect could still be a result of off-target inhibition of other MMPs. We stably expressed the ERK FRET sensor in the TACE-null cell line and analyzed ERK pulses in single cells. ERK activity is diminished and pulsatile ERK activity is largely eliminated by the loss of TACE (Figure 7C). These results suggest that TACE is required for generating pulsatile ERK activity, which correlates with the reduction in S-phase entry and cell proliferation demonstrated by TACE knockout HaCaT keratinocytes (Figure 3C).

DISCUSSION

We found that perturbing adherens junctions by depleting α-catenin elevates the release of the EGFR ligand TGF-α and reduces the requirement for exogenous growth factors for proliferation and migration. We show that TACE plays an essential role in the initiation and

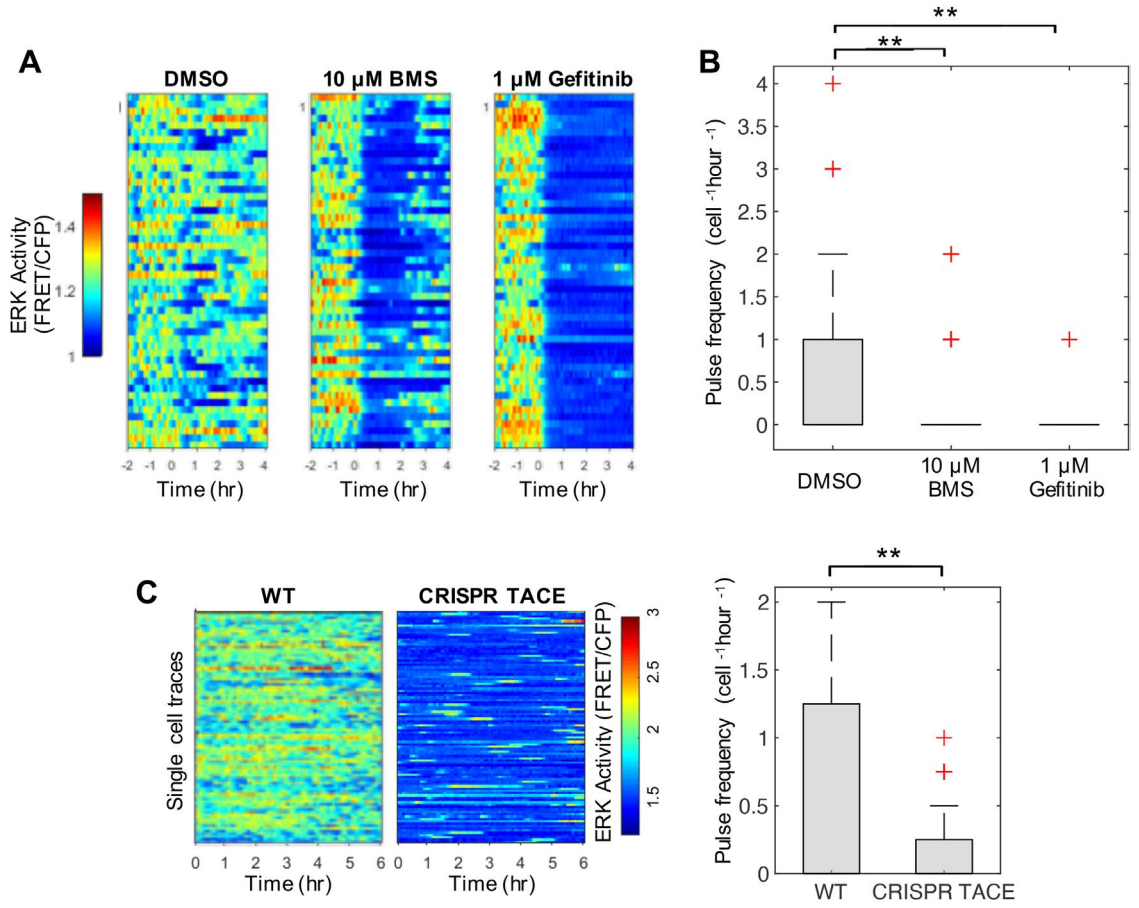

FIGURE 7: Pulsatile ERK activity in proliferating HaCaT keratinocytes requires TACE. (A) TACE inhibition disrupts pulsatile ERK activity. Each row displays a heatmap of ERK activity (FRET ratio of EKAR) for an individual HaCaT cell over time; 100 representative single-cell traces are shown. Cells were treated with 10 μM BMS, 1 μM gefitinib, or vehicle at 0 h. (B) Single-cell ERK pulses were counted over 1 h in triplicate wells with a custom MATLAB peak detection algorithm. One hundred fifty-four cells were quantified for DMSO, 156 for the BMS condition, and 166 for the gefitinib condition. (C) CRISPR TACE knockout HaCaT cells demonstrate diminished ERK pulses. One hundred representative single-cell traces of EKAR FRET ratio are displayed for wild-type (left) and CRISPR TACE knockout (right) cells. A large reduction in FRET ratio indicates lower ERK activity in TACE knockout cells. Single-cell ERK pulses were counted over 4 h in triplicate wells with a custom MATLAB peak detection algorithm, showing a large reduction in pulses upon knockout. One hundred twenty-three cells were quantified for wild type, 1666 for CRISPR TACE. In all panels, *p* values were determined by two-tailed Student's *t* test. ** $p \leq 0.0100$. Box plots show all data points with quartiles indicated; red crosses denote outliers.

maintenance of autocrine EGFR signaling in keratinocytes in response to growth factor stimulation and loss of α-catenin, because TACE knockout cells are defective in cell proliferation and migration without external EGF. Furthermore, we demonstrate that TACE is required for producing pulsatile ERK activity in keratinocyte cell clusters. Our results suggest that transient loss of cellular adherens junctions or reorganization of the junctional complex is most likely a trigger event for elevating autocrine signaling via TACE and that the feedback loop between TACE and the EGFR-ERK axis sustains TGF-α ligand production to promote proliferation and migration in keratinocytes.

The existence of positive TACE-ERK feedback has been well-recognized as a possible mechanism for autocrine signaling (Shvartsman *et al.*, 2002; Soond *et al.*, 2005; Le Gall *et al.*, 2010; Xu and Derynck, 2010; Dang *et al.*, 2013; Miller *et al.*, 2013; Arkun and Yasemi, 2018). However, the exact mechanism of TACE activation by ERK and the exact cellular context in which this positive feedback loop operates remain uncertain. Reports have shown that active ERK phosphorylates TACE at Thr-735, leading to TACE maturation and trafficking to the cell surface (Soond *et al.*, 2005; Xu and Derynck, 2010; Xu *et al.*, 2012). However, this model is at odds with several subsequent studies showing that ERK is capable of elevating the activity of mutant TACE without the cytosolic domain (Le Gall *et al.*, 2010; Schwarz *et al.*, 2013). Recent studies have identified the iRhom proteins (iRhom 1 and 2) as critical regulators of TACE maturation and activation (Adrain *et al.*, 2012; McIlwain *et al.*, 2012; Siggs *et al.*, 2014; Künzel *et al.*, 2018). iRhoms control the transport of TACE from the endoplasmic reticulum to the Golgi and remain in complex with TACE on the cell surface to form the sheddase complex that includes TACE, iRhom2, and FRMD8/iTAP (Künzel *et al.*, 2018; Oikonomidi *et al.*, 2018). One possible mechanism that may account for ERK-induced TACE activation is that ERK may phosphorylate iRhom2 to promote the proteolytic activity of TACE (Grieve *et al.*, 2017). Thus, ERK-induced activation of TACE may act directly through the phosphorylation of TACE or its partner iRhom2.

Our previous work showed that actin/cytoskeleton changes can promote TACE activity by increasing the presence of TACE on the cell surface independently of ERK and p38 (Chapnick *et al.*, 2015). The current study shows that loss of α-catenin and adherens junctions elevates TACE-dependent ligand shedding. Because α-catenin

serves both to generate a link between cadherin–cadherin junctions by binding actin and vinculin under tension (Rangarajan and Izard, 2013; Buckley *et al.*, 2014; Yao *et al.*, 2014) and to form homodimers capable of binding actin filaments (Drees *et al.*, 2005; Yamada *et al.*, 2005), reduction in α-catenin could, in theory, release Arp2/3 inhibition, thereby increasing actin dynamics at the cell membrane and activating TACE in a manner similar to that of cytochalasin D (a powerful activator of TACE in HaCaT cells) (Chapnick *et al.*, 2015). Alternatively, the morphological changes caused by silencing α-catenin are dramatic and likely accompanied by large-scale changes in cellular trafficking and the reorganization of membrane proteins, including the sheddase complex and pro-TGF-α. Finally, α-catenin has also been shown to inhibit transcription in the nucleus (Daugherty *et al.*, 2014). Loss of α-catenin may derepress transcription of certain genes that affect TACE activation directly or indirectly, although we did not see any changes in protein levels of TACE, c-MYC, ERK, and slug (Figures 4–6). Because TACE is a sheddase with more than 80 cellular substrates (Cavadas *et al.*, 2017), TACE regulation is highly complex. The underlying mechanism(s) for initiating this autocrine signaling cascade upon loss of α-catenin requires further investigation.

Pulsatile ERK activity has been observed in cultured mammalian cells and in the epidermis of living mice (Albeck *et al.*, 2013; Aoki *et al.*, 2013; Hiratsuka *et al.*, 2015, 2020; Johnson *et al.*, 2017; Ogura *et al.*, 2018). Oscillatory ERK activity is associated with cell proliferation (Albeck *et al.*, 2013; Aoki *et al.*, 2013). The mechanisms for the generation of ERK activity pulses are still debatable. Negative feedback from ERK to SOS1 (Cherniack *et al.*, 1995) or ERK to c-Raf (Dougherty *et al.*, 2005; Aoki *et al.*, 2013) or ERK modulation of DUSP6 and DUSP10 (Amit *et al.*, 2007; Hiratsuka *et al.*, 2020) have all been proposed. Consistent with these published results (Albeck *et al.*, 2013; Aoki *et al.*, 2013), we observed pulsatile ERK activity in keratinocytes that depends on both EGFR and TACE. Additionally, our studies with the TACE-null HaCaT cell line provide new genetic evidence that TACE is required for ERK oscillation, which correlates with S-phase entry and cell proliferation. This result suggests that TACE activity and production of the EGF family of ligands may also account for the generation of ERK activity pulses. Further studies are necessary to differentiate relevant extracellular and intercellular mechanisms for TACE-dependent ERK activity oscillation.

Sustained proliferative signaling is one of the hallmarks of cancer cells (Hanahan and Weinberg, 2011). We found that depletion of α-catenin reduces growth factor dependence as a result of autocrine production of TGF-α. A previous study showed that knocking out α-catenin in mouse epithelia causes a hyperproliferative phenotype within the skin, in which proliferation occurs in multiple layers resembling a squamous cell carcinoma (Vasioukhin *et al.*, 2001). Loss of epithelial cadherins and disruption of adherens junctions are associated with invasive tumors and cancer progression (Jeanes *et al.*, 2008; Yu *et al.*, 2019). Our result suggests that this hyperproliferative phenotype and enhanced motility could be a result of persistent autocrine activation of the EGFR-ERK pathway.

While persistent disruption of cellular junctions is associated with carcinogenesis, reversible weakening of cell–cell junctions may be co-opted to repair damaged epithelial sheets. Normal epidermal cells are nonmotile, but cells near wound edges undergo morphological changes and gain the ability to migrate to fill the gap between wound borders. Cells at the leading edge of an epithelial sheet have elevated receptor tyrosine kinase signaling and reorganize their cytoskeletons (Vitorino and Meyer, 2008). Keratinocytes with reduced expression of α-catenin share many similarities with these leader cells, and our results show that elevated TACE causes changes in ERK signaling that may be responsible for these similarities. A corollary to this notion is that reversible disruption of cell–cell junctions may be a therapeutic strategy for wound healing that could overcome the bioavailability problems associated with growth factor therapies. Future studies are needed to test whether this concept is translatable.

MATERIALS AND METHODS

Request a protocol through Bio-protocol.

Cell culture

HaCaT cells were cultured in DMEM supplemented with 2 mM L-glutamine, 100 U/ml penicillin, 100 U/ml streptomycin, and 10% (vol/vol) fetal bovine serum under 5% CO_2 at 37°C. HaCaT cells with a CRISPR/Cas9 knockout of TACE were additionally cultured in 6 pM EGF until TACE was rescued. Cell lines were authenticated by the American Type Culture Collection and regularly tested for mycoplasma infection.

Cell proliferation assays

Cells were exposed to 5-ethynyl-2′-deoxy-uridine (EdU) for 4 h before fixation with 4% paraformaldehyde for 5 min. Cells were then treated as per the instructions in the Click-IT EdU Alexa Fluor 647 Imaging Kit (Life Technologies) to determine the percentage of cells proliferating. Analysis was done with custom MATLAB scripts to determine the fraction of Hoechst nuclei positive for EdU stain. For assays performed on cells with CRISPR/Cas9 knockout of TACE, the cells were treated with media with EGF supplement for 5 d before treatment with EdU.

Western blotting

Whole-cell lysates of 1.25×10^6 cells in a six-well plate were prepared in radioimmunoprecipitation assay buffer (25 mM Tris-HCl [pH 7.4], 150 mM NaCl, 1% sodium deoxycholate, 1% Triton X-100, 0.1% SDS, 1 mM EDTA, 1 mM phenylmethylsulfonyl fluoride, 30 mM NaF, 1 mM sodium orthovanadate). Antibodies used for Western blots were against TACE (Ab39162; Abcam), Slug (9585T; Cell Signaling), vimentin (GTX100619; Genetex), ERK2 (sc-1647; Santa Cruz Biotechnology), p-ERK (sc-7383; Santa Cruz Biotechnology), α-tubulin (sc-12462; Santa Cruz Biotechnology), c-Myc (sc-40; Santa Cruz Biotechnology), αE-catenin (sc-7894; Santa Cruz Biotechnology), E-cadherin (sc-71008; Santa Cruz Biotechnology), N-cadherin (sc-393933; Santa Cruz Biotechnology), and GAPDH (sc-47724; Santa Cruz Biotechnology).

Neutralizing antibodies

Cetuximab was a gift from Gail Eckhardt (University of Texas at Austin's Dell Medical School), and anti–TGF-α (ab9585) was purchased from Abcam. These were used at 100 and 45 μg/ml, respectively.

Stable shRNA expression

Stable shRNA knockdown of α-catenin was achieved using TRC Lentiviral shRNA (ThermoFisher) with the construct TRCN0000234534 and nontargeting control SHC016 through lentiviral transduction. Cell lines were selected by 1 μg/ml puromycin treatment for 3 d. Lentiviral production was done in 293T cells with pHCMV-VSV-g, pMDLg, and pREV vectors.

CRISPR/Cas9 knockout

CRISPR/Cas9 knockout of TACE was performed by cloning the 20 base pair sequence 5′-CCAATTCATGAGTTGTAACC-3′ as the guide RNA into LentiCRISPR (pXPR_001) (Shalem *et al.*, 2014) and

using lentiviral transduction as a delivery system. The cells were then selected with 0.5 µg/ml puromycin for 3 d and allowed to recover in 6 pM EGF before they were diluted to a single cell per well in 96-well plates before being moved into larger dishes. Clonally expanded populations were measured for TACE levels by Western blot. TACE expression vector pRK5F-TACE was obtained from Addgene (#31713). The TACE coding sequence was subcloned into pEntry-MCS by PCR. For the rescue experiment, the TACE coding region corresponding to the sgRNA sequence was changed using a Quikchange site-specific mutagenesis kit (Agilent) by introducing silent mutations into the corresponding sgRNA targeting site (CCTAGCTCGTGAGTTGTAACC), which makes cells expressing the rescue clone resistant to CRISPR editing. The CRISPR-insensitive TACE was subcloned into mammalian expression destination vector pBbsr-Rfa-IRES-Blasticidin via Gateway cloning to yield pBbsr-TACEmut01. The destination vector was constructed by inserting the Rfa cassette into pPBbsr (Yusa *et al.*, 2009; Komatsu *et al.*, 2011). TACE rescue was achieved by cotransfection of pBbsr-TACEmut01 with mPB, which encodes the PB transposase (Yusa *et al.*, 2009). Blasticidin-resistant clones were selected for.

Fluorescent protein secretion experiments

mRuby2-Gluc-TGF-α secretion experiments were conducted by transferring the media from a 96-well plate (Costar) containing cells grown for 18 h to a 96-well PCR plate, centrifuging at 233 × *g* for 5 min, and then transferring 100 µl of the total 150 µl to a round-bottomed 96-well plate (Corning 4520). The fluorescence of the media was then measured using a Tecan Microplate reader with an excitation of 570/10 nm and an emission of 610/5 nm.

FRET data analysis and fluorescence spectroscopy

Cells were incubated and imaged in Corning 3603 96-well plates. Filters used for FRET measurements were the following: FRET excitation 438/24–25, dichroic 520LP, emission 542/27–25 (Semrock MOLE-0189); CFP excitation 438/24–25, dichroic 458LP, emission 483/32–25 (Semrock CFP- 2432B-NTE-Zero). Measurements were performed in triplicate with 10× magnification. For images displayed, 40× magnification was used.

Construction of a new TGF-α cleavage biosensor

A gene fragment with mRuby2-Gluc inserted between amino acids 41 and 42 of the TGF-α coding sequencing was chemically synthesized by SynBio Technologies (Monmouth Junction, NJ) and subcloned into a Gateway Entry vector with multiple cloning sites (pEntry-MCS) with *SalI-NotI*. The pEntry-mRuby2-Gluc-TGF-α was recombined with CSIV-Rfa-IRES-Hygromycin based on CSIV-Rfa-IRES-KT backbone (Isaji *et al.*, 2014) to derive the lentiviral reporter construct CSIV-mRuby2-Gluc-TGF-α for stable expression in mammalian cells.

Luciferase assays

Measurements of *Gaussia* luciferase signal in the media were performed using a GeneCopoeia Secrete-Pair *Gaussia* luciferase assay kit (Cat. LF061) according to the manufacturer protocol for use with the GL-S buffer. Samples were measured in a Nunc F96 MicroWell white plate on a Wallac Victor2 1420 Multilabel HTS Counter with an integration time of 1 s. The mean of three control wells containing substrate but no sample was subtracted from each measurement.

TGF-α ELISA

The media was collected from samples grown in six-well cell culture plates, spun at 200 RCF for 10 min, and passed through a 0.22 µm syringe filter. TGF-α levels were measured using an R&D Systems TGF-α Quantikine ELISA kit (Cat. DTGA00) according to the manufacturer protocol. Samples were measured on a Molecular Devices Spectramax iD3 multi-mode microplate reader.

Quantitative analysis of cell motility

Cell motility was assessed by processing nuclear dye image stacks with TrackMate (Tinevez *et al.*, 2017), which allows for determination of the median speed of the population average for each imaging site. TrackMate settings are as follows for 40× images: blob diameter of 30.0 pixels control for control shRNA cells and 20.0 pixels for α-catenin knockdown cells; threshold of 2.0; a max linking distance of 35.0 pixels; otherwise default settings. TrackMate settings are as follows for 10× images: blob diameter of 15.0 pixels; threshold of 12.0; a max linking distance of 15.0 pixels; otherwise default settings. Cells that were tracked over 12 or more consecutive time points were included in analysis. Analyses were performed using MATLAB and Excel; raw output files and analysis files are available upon request.

Analysis of ERK activity pulses

HaCaT cells expressing EKAR and stained with SiR DNA dye (Cytoskeleton) were tracked using custom MATLAB scripts. After single-cell traces of position, nuclear dye intensity, and FRET-to-CFP ratio were recorded, the pulse number could be quantified. Using MATLAB, cells were filtered by whether they underwent mitosis during the experiment by fitting the nuclear dye trace and removing cells with high relative values. Next a peak finding algorithm built into MATLAB was used to find high points of FRET-to-CFP ratio based on a height of 2 and prominence of 0.33 in a 1-h period. Peaks were normalized to the number of cells then reported at pulses per cell per hour.

ACKNOWLEDGMENTS

We thank Natalie Ahn, Amy Palmer, David Bortz, and Sabrina Spencer for advice and members of the Liu laboratory for discussion and suggestions. We thank Joseph Dragavon and the BioFrontiers Advanced Light Microscopy Core for their microscopy and imaging support. We thank Carl Blobel for sharing Adam 17 knockout MEFs, Hiroyuki Miyoshi for CSIV lentiviral vector, Allan Bradley for mPB, Kazuhiro Aoki and Michiyuki Matsuda for PiggyBac expression vector pBbsr, and Steven Wiley for MATLAB scripts. This work was supported by grants from the National Cancer Institute and the National Institute of Arthritis and Musculoskeletal and Skin Diseases of the National Institutes of Health (R01AR068254) to X. L. and National Institute of General Medical Sciences (NIGMS) R01GM126559 to David Bortz (University of Colorado Department of Applied Mathematics) and X. L. The content is solely the responsibility of the authors and does not necessarily represent the official views of the National Institutes of Health. E.N.B. and G.E.W. were supported by a predoctoral training grant from the NIGMS (T32GM08759). The ImageXpress MicroXL was supported by the National Center for Research Resources (S10 RR026680). FACSAria and the Opera Phenix imaging system were supported by the National Institutes of Health (S10OD021601 and S10OD025072).

REFERENCES

Adrain C, Zettl M, Christova Y, Taylor N, Freeman M (2012). Tumor necrosis factor signaling requires iRhom2 to promote trafficking and activation of TACE. Science 335, 225–228.

Albeck JG, Mills GB, Brugge JS (2013). Frequency-modulated pulses of ERK activity transmit quantitative proliferation signals. Mol Cell 49, 249–261.

Amit I, Citri A, Shay T, Lu Y, Menachem K, Zhang F, Tarcic G, Siwak D, Lahad J, Jacob-Hirsch J, *et al.* (2007). A module of negative feedback regulators defines growth factor signaling. Nat Genet 39, 503–512.

Aoki K, Kondo Y, Naoki H, Hiratsuka T, Itoh RE, Matsuda M (2017). Propagating wave of ERK activation orients collective cell migration. Dev Cell 43, 305–317.e5.
Aoki K, Kumagai Y, Sakurai A, Komatsu N, Fujita Y, Shionyu C, Matsuda M (2013). Stochastic ERK activation induced by noise and cell-to-cell propagation regulates cell density-dependent proliferation. Mol Cell 52, 529–540.
Arkun Y, Yasemi M (2018). Dynamics and control of the ERK signaling pathway: sensitivity, bistability, and oscillations. PLoS One 13, 1–24.
Blobel CP (2005). ADAMs: key components in EGFR signalling and development. Nat Rev Mol Cell Biol 6, 32–43.
Borrell-Pagès M, Rojo F, Albanell J, Baselga J, Arribas J (2003). TACE is required for the activation of the EGFR by TGF-alpha in tumors. EMBO J 22, 1114–1124.
Brandner JM, Haftek M, Niessen CM (2010). Adherens junctions, desmosomes and tight junctions in epidermal barrier function. Open Dermatol J 4, 14–20.
Buckley CD, Tan J, Anderson KL, Hanein D, Volkmann N, Weis WI, Nelson WJ, Dunn AR (2014). The minimal cadherin-catenin complex binds to actin filaments under force. Science 346, 1254211–1254218.
Cavadas M, Oikonomidi I, Gaspar C, Burbridge E, Badenes M, Félix I, Bolado A, Hu T, Bileck A, Gerner G, *et al*. (2017). Phosphorylation of iRhom2 controls stimulated proteolytic shedding by the metalloprotease ADAM17/TACE. Cell Rep 21, 745–757.
Chapnick DA, Bunker E, Liu X (2015). A biosensor for the activity of the "sheddase" TACE (ADAM17) reveals novel and cell type-specific mechanisms of TACE activation. Sci Signal 8, rs1.
Chapnick DA, Liu X (2014). Leader cell positioning drives wound-directed collective migration in TGFβ-stimulated epithelial sheets. Mol Biol Cell 25, 1586–1593.
Cherniack AD, Klarlund JK, Conway BR, Czech MP (1995). Disassembly of Son-of-sevenless proteins from Grb2 during p21 desensitization by insulin. J Biol Chem 270, 1485–1488.
Dang M, Armbruster N, Miller MA, Cermeno E, Hartmann M, Bell GW, Root DE, Lauffenburger DA, Lodish HF, Herrlich A (2013). Regulated ADAM17-dependent EGF family ligand release by substrate-selecting signaling pathways. Proc Natl Acad Sci USA 110, 9776–9781.
Daugherty RL, Serebryannyy L, Yemelyanov A, Flozak AS, Yu H-J, Kosak ST, deLanerolle P, Gottardi CJ (2014). α-Catenin is an inhibitor of transcription. Proc Natl Acad Sci USA 111, 5260–5265.
Dougherty MK, Müller J, Ritt DA, Zhou M, Zhou XZ, Copeland TD, Conrads TP, Veenstra TD, Lu KP, Morrison DK (2005). Regulation of Raf-1 by direct feedback phosphorylation. Mol Cell 17, 215–224.
Drees F, Pokutta S, Yamada S, Nelson WJ, Weis WI (2005). α-Catenin is a molecular switch that binds E-cadherin-β-catenin and regulates actin-filament assembly. Cell 123, 903–915.
Fuchs E, Raghavan S (2002). Getting under the skin of epidermal morphogenesis. Nat Rev Genet 3, 199–209.
Grieve AG, Xu H, Künzel U, Bambrough P, Sieber B, Freeman M (2017). Phosphorylation of iRhom2 at the plasma membrane controls mammalian TACE-dependent inflammatory and growth factor signalling. eLife 6, e23968.
Grootveld M, McDermott MF (2003). BMS-561392. Bristol-Myers Squibb. Curr Opin Investig Drugs 4, 598–602.
Gurtner GC, Werner S, Barrandon Y, Longaker MT (2008). Wound repair and regeneration. Nature 453, 314–321.
Hanahan D, Weinberg RA (2011). Hallmarks of cancer: the next generation. Cell 144, 646–674.
Harris RC, Chung E, Coffey RJ (2003). EGF receptor ligands. Exp Cell Res 284, 2–13.
Harvey CD, Ehrhardt AG, Cellurale C, Zhong H, Yasuda R, Davis RJ, Svoboda K (2008). A genetically encoded fluorescent sensor of ERK activity. Proc Natl Acad Sci USA 105, 19264–19269.
Hiratsuka T, Bordeu I, Pruessner G, Watt FM (2020). Regulation of ERK basal and pulsatile activity control proliferation and exit from the stem cell compartment in mammalian epidermis. Proc Natl Acad Sci USA 117, 17796–17807.
Hiratsuka T, Fujita Y, Naoki H, Aoki K, Kamioka Y, Matsuda M (2015). Intercellular propagation of extracellular signal-regulated kinase activation revealed by in vivo imaging of mouse skin. eLife 4, e05178.
Isaji T, Im S, Gu W, Wang Y, Hang Q, Lu J, Fukuda T, Hashii N, Takakura D, Kawasaki N, *et al*. (2014). An oncogenic protein Golgi phosphoprotein 3 up-regulates cell migration via sialylation. J Biol Chem 289, 20694–20705.
Jeanes A, Gottardi C, Yap A (2008). Cadherins and cancer: how does cadherin dysfunction promote tumor progression? Oncogene 27, 6920–6929.
Johnson HE, Goyal Y, Pannucci NL, Schüpbach T, Shvartsman SY, Toettcher JE (2017). The spatiotemporal limits of developmental Erk signaling. Dev Cell 40, 185–192.
Komatsu N, Aoki K, Yamada M, Yukinaga H, Fujita Y, Kamioka Y, Matsuda M (2011). Development of an optimized backbone of FRET biosensors for kinases and GTPases. Mol Biol Cell 22, 4647–4656.
Künzel U, Grieve AG, Meng Y, Sieber B, Cowley SA, Freeman M (2018). FRMD8 promotes inflammatory and growth factor signalling by stabilising the iRhom/ADAM17 sheddase complex. eLife 7, e35012.
Le Gall SM, Bobe P, Reiss K, Horiuchi K, Niu X-D, Lundell D, Gibb DR, Conrad D, Saftig P, Blobel CP (2009). ADAMs 10 and 17 represent differentially regulated components of a general shedding machinery for membrane proteins such as transforming growth factor, L-selectin, and tumor necrosis factor. Mol Biol Cell 20, 1785–1794.
Le Gall SM, Maretzky T, Issuree PDA, Niu X-D, Reiss K, Saftig P, Khokha R, Lundell D, Blobel CP (2010). ADAM17 is regulated by a rapid and reversible mechanism that controls access to its catalytic site. J Cell Sci 123, 3913–3922.
Lee DC, Sunnarborg SW, Hinkle CL, Myers TJ, Stevenson MY, Russell WE, Castner BJ, Gerhart MJ, Paxton RJ, Black RA, *et al*. (2003). TACE/ADAM17 processing of EGFR ligands indicates a role as a physiological convertase. Ann NY Acad Sci 995, 22–38.
Maretzky T, Zhou W, Huang XY, Blobel CP (2011). A transforming Src mutant increases the bioavailability of EGFR ligands via stimulation of the cell-surface metalloproteinase ADAM17. Oncogene 30, 611–618.
McIlwain DR, Lang PA, Maretzky T, Hamada K, Ohishi K, Maney SK, Berger T, Murthy A, Duncan G, Xu HC, et al. (2012). iRhom2 regulation of TACE controls TNF-mediated protection against Listeria and responses to LPS. Science 335, 229–232.
Miller MA, Meyer AS, Michael MT, Lasisi Z, Reddy S, Jeng KW, Chen C-H, Han J, Isaacson K, Griffith LG, Lauffenburger DA. (2013). ADAM-10 and -17 regulate endometriotic cell migration via concerted ligand and receptor shedding feedback on kinase signaling. Proc Natl Acad Sci USA 110, E2074–E2083.
Nardini JT, Chapnick DA, Liu X, Bortz DM (2016). Modeling keratinocyte wound healing dynamics: cell-cell adhesion promotes sustained collective migration. J Theor Biol 400, 103–117.
Ogura Y, Wen F-L, Sami MM, Shibata T, Hayashi S (2018). A switch-like activation relay of EGFR-ERK signaling regulates a wave of cellular contractility for epithelial invagination. Dev Cell 46, 162–172.e5.
Oikonomidi I, Burbridge E, Cavadas M, Sullivan G, Collis B, Naegele H, Clancy D, Brezinova J, Hu T, Bileck A, *et al*. (2018). iTAP, a novel iRhom interactor, controls TNF secretion by policing the stability of iRhom/TACE. eLife 7, 13.
Pastar I, Stojadinovic O, Yin NC, Ramirez H, Nusbaum AG, Sawaya A, Patel SB, Khalid L, Isseroff RR, Tomic-Canic M (2014). Epithelialization in wound healing: a comprehensive review. Adv Wound Care 3, 445–464.
Peschon JJ, Slack JL, Reddy P, Stocking KL, Sunnarborg SW, Lee DC, Russell WE, Castner BJ, Johnson RS, Fitzner JN, *et al*. (1998). An essential role for ectodomain shedding in mammalian development. Science 282, 1281–1284.
Rangarajan ES, Izard T (2013). Dimer asymmetry defines α-catenin interactions. Nat Struct Mol Biol 20, 188–193.
Regot S, Hughey JJ, Bajar BT, Carrasco S, Covert MW (2014). High-sensitivity measurements of multiple kinase activities in live single cells. Cell 157, 1724–1734.
Sahin U, Blobel CP (2007). Ectodomain shedding of the EGF-receptor ligand epigen is mediated by ADAM17. FEBS Lett 581, 41–44.
Scheller J, Chalaris A, Garbers C, Rose-John S (2011). ADAM17: a molecular switch to control inflammation and tissue regeneration. Trends Immunol 32, 380–387.
Schwarz J, Broder C, Helmstetter A, Schmidt S, Yan I, Müller M, Schmidt-Arras D, Becker-Pauly C, Koch-Nolte F, Mittrücker H-W, *et al*. (2013). Short-term TNFα shedding is independent of cytoplasmic phosphorylation or furin cleavage of ADAM17. Biochim Biophys Acta 1833, 3355–3367.
Shalem O, Sanjana NE, Hartenian E, Shi X, Scott DA, Mikkelsen TS, Heckl D, Ebert BL, Root DE, Doench JG, Zhang F (2014). Genome-scale CRISPR-Cas9 knockout screening in human cells. Science 343, 84–87.
Shvartsman SY, Hagan MP, Yacoub A, Dent P, Wiley HS, Lauffenburger DA (2002). Autocrine loops with positive feedback enable context-dependent cell signaling. Am J Physiol Cell Physiol 282, C545–C559.

Siggs OM, Grieve A, Xu H, Bambrough P, Christova Y, Freeman M (2014). Genetic interaction implicates iRhom2 in the regulation of EGF receptor signalling in mice. Biol Open 3, 1151–1157.
Soond SM, Everson B, Riches DW, Murphy G (2005). ERK-mediated phosphorylation of Thr735 in TNFalpha-converting enzyme and its potential role in TACE protein trafficking. J Cell Sci 118, 2371–2380.
Sparta B, Pargett M, Minguet M, Distor K, Bell G, Albeck JG (2015). Receptor level mechanisms are required for epidermal growth factor (EGF)-stimulated extracellular signal-regulated kinase (ERK) activity pulses. J Biol Chem 290, 24784–24792.
Tanimura S, Takeda K (2017). ERK signalling as a regulator of cell motility. J Biochem 162, 145–154.
Tinevez J-Y, Perry N, Schindelin J, Hoopes GM, Reynolds GD, Laplantine E, Bednarek SY, Shorte SL, Eliceiri KW (2017). TrackMate: an open and extensible platform for single-particle tracking. Methods 115, 80–90.
Vasioukhin V, Bauer C, Degenstein L, Wise B, Fuchs E (2001). Hyperproliferation and defects in epithelial polarity upon conditional ablation of α-catenin in skin. Cell 104, 605–617.
Vitorino P, Meyer T (2008). Modular control of endothelial sheet migration. Genes Dev 22, 3268–3281.
Wickert LE, Pomerenke S, Mitchell I, Masters KS, Kreeger PK (2016). Hierarchy of cellular decisions in collective behavior: implications for wound healing. Sci Rep 6, 1–9.
Xu J, Lamouille S, Derynck R (2009). TGF-β-induced epithelial to mesenchymal transition. Cell Res 19, 156–172.
Xu P, Derynck R (2010). Direct activation of TACE-mediated ectodomain shedding by p38 MAP kinase regulates EGF receptor-dependent cell proliferation. Mol Cell 37, 551–566.
Xu P, Liu J, Sakaki-Yumoto M, Derynck R (2012). TACE activation by MAPK-mediated regulation of cell surface dimerization and TIMP3 association. Sci Signal 5, ra34.
Yamada S, Pokutta S, Drees F, Weis WI, Nelson WJ (2005). Deconstructing the cadherin-catenin-actin complex. Cell 123, 889–901.
Yao M, Qiu W, Liu R, Efremov AK, Cong P, Seddiki R, Payre M, Lim CT, Ladoux B, Mége R-M, Yan J (2014). Force-dependent conformational switch of α -catenin controls vinculin binding. Nat Commun 5, 4525.
Yu W, Yang L, Li T, Zhang Y (2019). Cadherin signaling in cancer: its functions and role as a therapeutic target. Front Oncol 9, 989.
Yusa K, Rad R, Takeda J, Bradley A (2009). Generation of transgene-free induced pluripotent mouse stem cells by the piggyBac transposon. Nat Methods 6, 363–369.